Higher-order simplicial synchronization of coupled topological signals

Reza Ghorbanchian,[1] Juan G. Restrepo,[2] Joaquín J. Torres,[3] and Ginestra Bianconi[1,4]

[1]*School of Mathematical Sciences, Queen Mary University of London, London, E1 4NS, United Kingdom*
[2]*Department of Applied Mathematics, University of Colorado at Boulder, Boulder, CO 80309, USA*
[3]*Departamento de Electromagnetismo y Física de la Materia and Instituto Carlos I de Física Teórica y Computacional,*
Universidad de Granada, 18071, Granada, Spain
[4] *The Alan Turing Institute, The British Library, London, United Kingdom*

Simplicial complexes capture the underlying network topology and geometry of complex systems ranging from the brain to social networks. Representing complex systems as simplicial complexes opens the possibility to use the powerful tools of algebraic topology to characterize their structure. Here we show that algebraic topology can also be a fundamental tool to capture the higher-order dynamics of simplicial complexes. In particular we consider topological signals, i.e., dynamical signals defined on simplices of different dimension, here taken to be nodes and links for simplicity. We use algebraic topology for characterizing the coupled dynamics of topological signals defined on nodes and links. This dynamical process is ideally suited for simplicial complexes but might also be used to treat topological dynamics on networks with exclusively pairwise interactions. We show that this coupled synchronization leads to explosive topological synchronization in which phases defined on nodes synchronize simultaneously to phases defined on links at a discontinuous phase transition. The model is here studied on real connectomes and on simplicial network models. Finally, we provide a comprehensive theoretical approach that captures this transition on random networks treated within the annealed approximation.

I. INTRODUCTION

Higher-order networks [1–4] are attracting increasing attention as they are able to capture the many-body interactions of complex systems ranging from brain to social networks. Simplicial complexes are higher-order networks that encode the network geometry and topology of real datasets. Using simplicial complexes allows the network scientist to formulate new mathematical frameworks for mining data [5–10] and for understanding these generalized network structures revealing the underlying deep physical mechanisms for emergent geometry [11–15] and for higher-order dynamics [16–33]. In particular, this very vibrant research activity is relevant in brain research to analyse real brain data and its profound relation to brain dynamics [1, 6, 15, 34–37] and in biology, e.g., for the study of biological transport networks [10, 38].

In networks, dynamical processes are typically defined over signals associated to the nodes of the network. In particular, the Kuramoto model [39–43] investigates the synchronization transitions of phases associated to the nodes of the network. This scenario can change significantly in the case of simplicial complexes [16, 17, 19]. In fact, simplicial complexes can sustain dynamical signals defined on simplices of different dimension, including nodes, links, triangles and so on, called *topological signals*. For instance, topological signals defined on links can represent fluxes of interest in brain research and in biological transportation networks as well. The interest on topological signals is rapidly growing with new results related to signal processing of topological signals [17, 19] and higher-order topological synchronization [16, 28]. In particular higher-order topological synchronization [16] demonstrates that topological signals (phases) associated to higher dimensional simplices can undergo a synchro-

nization phase transition. Interestingly this synchronization transition can go unnoticed if the dynamics is not processed with the suitable topological transformations. These results open new uncharted territory for the investigation of higher-order synchronization.

Here we build on the mathematical framework of higher-order topological synchronization proposed in Ref. [16] and consider a synchronization model in which topological signals of different dimension are coupled. We focus in particular on the coupled synchronization of topological signals defined on nodes and links, but we note that the model can be easily extended to topological signals of higher dimension. The reason why we focus on topological signals defined on nodes and links is threefold. First of all we can have a better physical intuition of topological signals defined on nodes (traditionally studied by the Kuramoto model) and links (like fluxes) that is relevant in brain dynamics [44] and biological transport networks [10, 38]. Secondly, although the coupled synchronization dynamics of nodes and links can be considered as a special case of coupled synchronization dynamics of higher-order topological signals on a generic simplicial complex, this dynamics can be observed also on networks including only pairwise interactions. Indeed nodes and links are the simplices that remain unchanged if we reduce a simplicial complex to its network skeleton. Since currently there is more availability of network data than simplicial complex data, this fact implies that the coupled dynamics studied in this work has wide applicability as it can be tested on any network data and network model. Thirdly, defining the coupled dynamics of topological signals defined on nodes and links can open new perspectives in exploiting the properties of the line graph of a given network which is the network whose nodes corresponds to the links or the original network
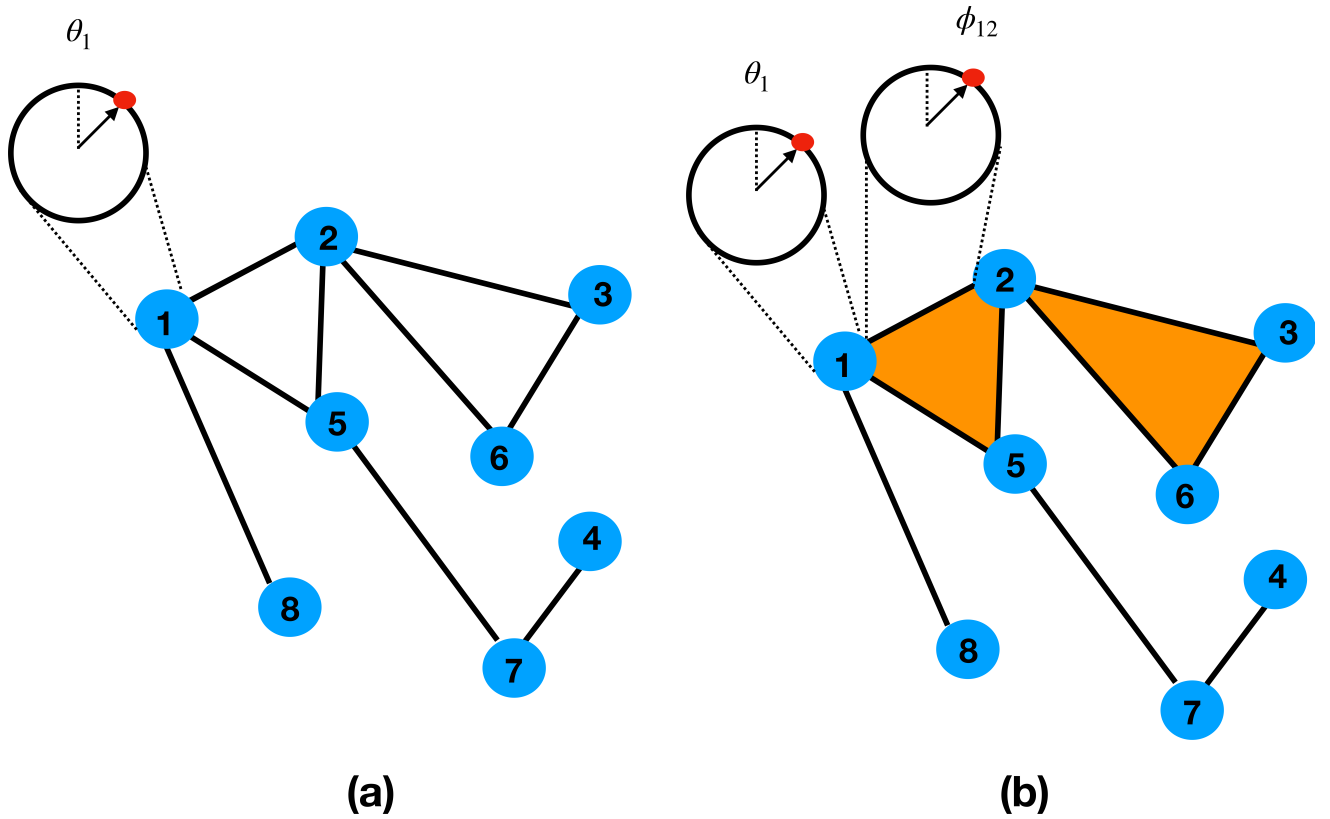
FIG. 1: **Schematic representation of the Kuramoto and the topological Kuramoto model.** Panel (a) shows a network in which nodes sustain a dynamical variable (a phase) whose synchronization is captured by the Kuramoto model. Panel (b) shows a simplicial complex in which not only nodes but also links sustain dynamical variables whose coupled synchronization dynamics is captured by the higher-order topological Kuramoto model.

[45].

In this work, we show that by adopting a global adaptive coupling of dynamics inspired by Refs. [46, 47] the coupled synchronization dynamics of topological signals defined on nodes and links is explosive [48], i.e., it occurs at a discontinuous phase transition in which the two topological signals of different dimension synchronize at the same time. We also illustrate numerical evidence of this discontinuity on real connectomes and on simplicial complex models including the configuration model of simplicial complexes [49] and the non-equilibrium simplicial complex model called Network Geometry with Flavor [12, 13]. We provide a comprehensive theory of this phenomenon formulated within the annealed network approximation of random networks offering a good analytical understanding of the observed transition. The analytical results give solid ground to the claim that the investigated transition is discontinuous.

II. SIMPLICIAL COMPLEXES AND HIGHER ORDER LAPLACIANS

A. Definition of simplicial complexes

Simplicial complexes represent higher-order networks whose interactions include two or more nodes. These many-body interactions are captured by *simplices*. A n-dimensional *simplex* α is a set of $n + 1$ nodes

$$\alpha = [i_0, i_1, \ldots, i_n]. \tag{1}$$

For instance a node is a 0-dimensional simplex, a link is a 1-dimensional simplex, a triangle is a 2-dimensional simplex, a tetrahedron is a 3-dimensional simplex, and so on. A *face* of a simplex is the simplex formed by a proper subset of the nodes of the original simplex. For instance the faces of a tetrahedron are 4 nodes, 6 links and 4 triangles. A *simplicial complex* is a set of simplices closed under the inclusion of the faces of each simplex. Any simplicial complex can be reduced to its *simplicial complex skeleton*, which is the network formed by the simplicial complex nodes and links. Simplices have a relevant topological and geometrical interpretation and constitute the topological structures studied by discrete algebraic topology. Therefore representing the many-body

Boundary operator

(a)

$$\partial_1[1,2] = [2] - [1]\,.$$

(b)

$$\partial_2[1,2,3] = [2,3] - [1,3] + [1,2]\,.$$

Incidence matrices

(c)

(d)

$$\mathbf{B}_{[1]} = \begin{array}{c|cccc} & [1,2] & [1,3] & [2,3] & [3,4] \\ \hline [1] & -1 & -1 & 0 & 0 \\ [2] & 1 & 0 & -1 & 0 \\ [3] & 0 & 1 & 1 & -1 \\ [4] & 0 & 0 & 0 & 1 \end{array},$$

$$\mathbf{B}_{[2]} = \begin{array}{c|c} & [1,2,3] \\ \hline [1,2] & 1 \\ [1,3] & -1 \\ [2,3] & 1 \\ [3,4] & 0 \end{array}.$$
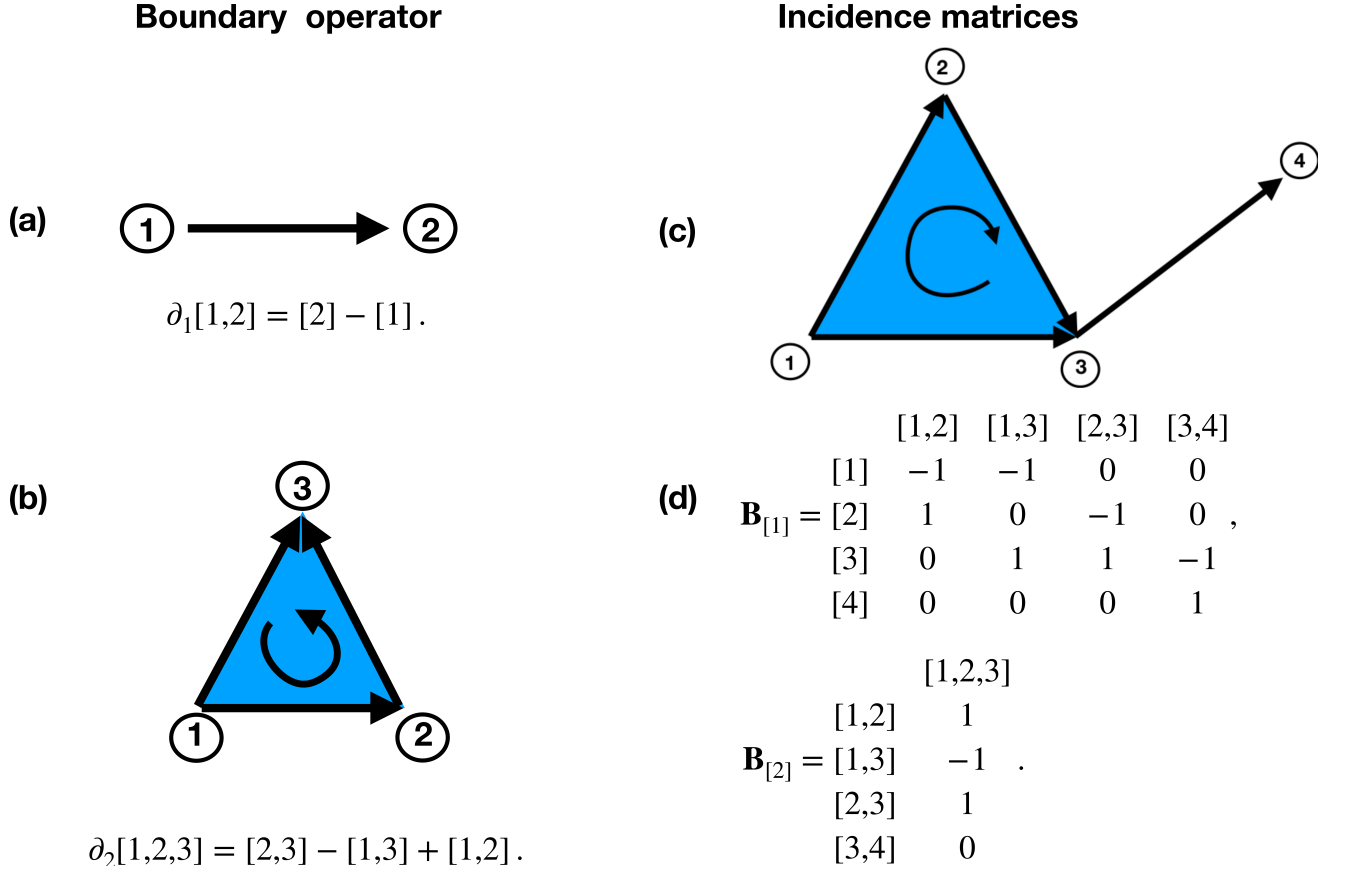
FIG. 2: **The boundary operators and their representation in terms of the incidence matrices.** Panel (a) and (b) describe the action of the boundary operator on an oriented link and on an oriented triangle respectively. Panel (c) shows a toy example of a simplicial complex and panel (d) indicates its incidence matrices $\mathbf{B}_{[1]}$ and $\mathbf{B}_{[2]}$ representing the boundary operators ∂_1 and ∂_2 respectively.

interactions of a complex system with a simplicial complex opens the very fertile opportunity to use the tools of algebraic topology [5, 50] to study the topology of the system under investigation. In this work we show that algebraic topology can also shed significant light on the role that topology has on higher-order synchronization.

B. Oriented simplices and boundary map

In algebraic topology simplices are oriented. For instance a link $\alpha = [i,j]$ has the opposite sign of the link $[j,i]$, i.e.,

$$[i,j] = -[j,i]. \tag{2}$$

Similarly to higher order simplices we associate an orientation such that

$$[i_0, i_1, \ldots, i_n] = (-1)^{\sigma(\pi)}[i_{\pi(0)}, i_{\pi(1)}, \ldots, i_{\pi(n)}], \tag{3}$$

where $\sigma(\pi)$ indicates the parity of the permutation π. It is good practice to use as orientation of the simplices the orientation induced by the labelling of the nodes, i.e.,

giving, for example, a positive orientation to any simplex

$$[i_0, i_1, \ldots, i_n], \tag{4}$$

where

$$i_0 < i_1 < i_2 \ldots < i_n. \tag{5}$$

This will ensure that the spectral properties of the higher-order Laplacians that will be defined later are independent of the labelling of the nodes. Given a simplicial complex, a n-chain consists of the elements of a free abelian group $\mathcal{C}_n$ with basis formed by the set of all oriented n-simplices. Therefore every element of $\mathcal{C}_n$ can be uniquely expressed as a linear combination of the basis elements (n-simplices) with coefficients in $\mathbb{Z}_2$. The boundary operator ∂_n is a linear operator $\partial_n : \mathcal{C}_n \to \mathcal{C}_{n-1}$ whose action is determined by the action on each n-simplex of the simplicial complex given by

$$\partial_n[i_0, i_1 \ldots, i_n] = \sum_{p=0}^{n} (-1)^p [i_0, i_1, \ldots, i_{p-1}, i_{p+1}, \ldots, i_n]. \tag{6}$$

As a concrete example, in Figure 2 we demonstrate the action of the boundary operator on links and triangles.

A celebrated property of the boundary operator is that the *boundary of a boundary is null*, i.e.

$$\partial_n \partial_{n+1} = 0 \qquad (7)$$

for any $n > 0$. This relation can be directly proven by using Eq. (6). Let us consider a simplicial complex $\mathcal{K}$. Let us indicate with $N_{[n]}$ the number of simplices of the simplicial complex with generic dimension n. Given a basis for the linear space of n-chains $\mathcal{C}_n$ and for the linear space of $(n-1)$-chains $\mathcal{C}_{n-1}$ formed by an ordered list of the n simplices and $(n-1)$ simplices of the simplicial complex, the boundary operator ∂_n can be represented as $N_{[n-1]} \times N_{[n]}$ incidence matrix $\mathbf{B}_{[n]}$. In Figure 2 we show a 2-dimensional simplicial complex and its corresponding incidence matrices $\mathbf{B}_{[1]}$ and $\mathbf{B}_{[2]}$. Given that the boundary matrices obey Eq. (7) it follows that the incidence matrices obey

$$\mathbf{B}_{[n]}\mathbf{B}_{[n+1]} = \mathbf{0}, \ \ \mathbf{B}_{[n+1]}^{\top}\mathbf{B}_{[n]}^{\top} = \mathbf{0}, \qquad (8)$$

for any $n > 0$.

C. Higher order Laplacians

Using the incidence matrices it is natural to generalize the definition of the graph Laplacian

$$\mathbf{L}_{[0]} = \mathbf{B}_{[1]}\mathbf{B}_{[1]}^{\top} \qquad (9)$$

to the higher-order Laplacian $\mathbf{L}_{[n]}$(also called combinatorial Laplacians) [17, 19, 51] that can be represented as a $N_{[n]} \times N_{[n]}$ matrix given by

$$\mathbf{L}_{[n]} = \mathbf{L}_{[n]}^{down} + \mathbf{L}_{[n]}^{up} \qquad (10)$$

with

$$\begin{aligned}\mathbf{L}_{[n]}^{down} &= \mathbf{B}_{[n]}^{\top}\mathbf{B}_{[n]}, \\ \mathbf{L}_{[n]}^{up} &= \mathbf{B}_{[n+1]}\mathbf{B}_{[n+1]}^{\top},\end{aligned} \qquad (11)$$

for $n > 0$. The higher-order Laplacian can be proven to be independent of the orientation of the simplices as long as the simplicial complex has an orientation induced by a labelling of the nodes.

The most celebrated property of higher-order Laplacian is that the degeneracy of the zero eigenvalue of the n Laplacian $\mathbf{L}_{[n]}$ is equal to the Betti number β_n and that their corresponding eigenvectors localize around the corresponding n-dimensional cavities of the simplicial complex. The higher-order Laplacians can be used to define higher-order diffusion [17] and can display a higher-order spectral dimension on network geometries. Here we are particularly interested in the use of incidence matrices and higher-order Laplacians to define higher-order topological synchronization.

III. HIGHER-ORDER TOPOLOGICAL SYNCHRONIZATION

A. Higher-order topological Kuramoto model of topological signals of a given dimension

The Kuramoto dynamics describes the synchonization transition for phases

$$\boldsymbol{\theta} = (\theta_1, \theta_2, \dots \theta_{N_{[0]}}) \qquad (12)$$

associated to nodes, i.e., simplices of dimension $n = 0$. The Kuramoto model is typically defined on a network but it can treat also synchronization of the phases associated to the nodes of a simplicial complex. Each node i has associated an internal frequency ω_i drawn from a given distribution, for instance a normal distribution $\omega_i \sim \mathcal{N}(\Omega_0, 1)$. In absence of any coupling, i.e., in absence of pairwise interactions, every node oscillates at its own frequency. However in a network or in a simplicial complex skeleton the phases associated to the nodes follow the dynamical evolution dictated by the equation

$$\dot{\boldsymbol{\theta}} = \boldsymbol{\omega} - \sigma\mathbf{B}_{[1]}\sin\left(\mathbf{B}_{[1]}^{\top}\boldsymbol{\theta}\right), \qquad (13)$$

where here and in the following we use the notation $\sin(\mathbf{x})$ to indicate the column vector where the sine function is taken element wise. Note that here we have chosen to write this system of equations in terms of the incidence matrix $\mathbf{B}_{[1]}$. However if we indicate with $\mathbf{a}$ the adjacency matrix of the network and with a_{ij} its matrix elements, this system of equations is equivalent to

$$\dot{\theta}_i = \omega_i + \sigma\sum_{j=1}^{N} a_{ij}\sin(\theta_j - \theta_i), \qquad (14)$$

valid for every node i of the network. For coupling constant $\sigma = \sigma_c$ the Kuramoto model [39–41] displays a continuous phase transition above which the order parameter

$$R_0 = \frac{1}{N_{[0]}}\left|\sum_{i=1}^{N_{[0]}} e^{i\theta_i}\right| \qquad (15)$$

is non-zero also in the limit $N_{[0]} \to \infty$. The higher-order topological Kuramoto model [16] describes synchronization of phases associated to the n dimensional simplices of a simplicial complex. Although the definition of the model applies directly to any value of n, here we consider specifically the case in which the higher-order Kuramoto model is defined on topological signals (phases) associated to the links

$$\boldsymbol{\phi} = (\phi_{\ell_1}, \phi_{\ell_2}, \dots \phi_{\ell_{N_{[1]}}}). \qquad (16)$$

In particular here ϕ_{ℓ_r} indicates the phase associated to the r-th link of the simplicial complex. The higher order

Kuramoto dynamics defined on simplices of dimension $n > 0$ is the natural extension of the standard Kuramoto model defiend by Eq. (13). Let us indicate with $\tilde{\boldsymbol{\omega}}$ the internal frequencies associated to the links of the simplicial complex, sampled for example from a normal distribution, $\tilde{\omega}_\ell \sim \mathcal{N}(\Omega_1, 1)$. The higher-order topological Kuramoto model is defined as

$$\dot{\boldsymbol{\phi}} = \tilde{\boldsymbol{\omega}} - \sigma \mathbf{B}_{[1]}^\top \sin(\mathbf{B}_{[1]}\boldsymbol{\phi}) - \sigma \mathbf{B}_{[2]} \sin(\mathbf{B}_{[2]}^\top \boldsymbol{\phi}). \quad (17)$$

Once the synchronization dynamics is defined on higher-order topological signals of dimension n (here taken to be $n = 1$) an important question is whether this dynamics can be projected on $(n+1)$ and $(n-1)$ simplices. Interestingly, algebraic topology provides a clear solution to this question. Indeed for $n = 1$, when the dynamics describes the evolution of phases associated to the links, one can consider the projection $\boldsymbol{\phi}^{[-]}$ and $\boldsymbol{\phi}^{[+]}$ respectively on nodes and on triangles defined as

$$\boldsymbol{\phi}^{[-]} = \mathbf{B}_{[1]}\boldsymbol{\phi},$$
$$\boldsymbol{\phi}^{[+]} = \mathbf{B}_{[2]}^\top \boldsymbol{\phi}. \quad (18)$$

Note that in this case $\mathbf{B}_{[1]}$ acts as a discrete divergence and $\mathbf{B}_{[2]}^\top$ acts as a discrete curl. Interestingly, since the incidence matrices satisfy Eq. (8) these two projected phases follow the uncoupled dynamics

$$\dot{\boldsymbol{\phi}}^{[-]} = \mathbf{B}_{[1]}\tilde{\boldsymbol{\omega}} - \sigma \mathbf{L}_{[0]} \sin \boldsymbol{\phi}^{[-]},$$
$$\dot{\boldsymbol{\phi}}^{[+]} = \mathbf{B}_{[2]}^\top \tilde{\boldsymbol{\omega}} - \sigma \mathbf{L}_{[2]}^{down} \sin \boldsymbol{\phi}^{[+]}. \quad (19)$$

These two projected dynamics undergo a continuous synchronization transition at $\sigma_c = 0$ [16] with order parameters

$$R_1^{down} = \frac{1}{N_{[0]}} \left| \sum_{i=1}^{N_{[0]}} e^{\hat{\imath}\phi_i^{[-]}} \right|,$$

$$R_1^{up} = \frac{1}{N_{[2]}} \left| \sum_{i=1}^{N_{[2]}} e^{\hat{\imath}\phi_i^{[+]}} \right|. \quad (20)$$

In Ref. [16] an adaptive coupling between these two dynamics is considered formulating the explosive higher-order topological Kuramoto model in which the topological signal follows the set of coupled equations

$$\dot{\boldsymbol{\phi}} = \tilde{\boldsymbol{\omega}} - \sigma R_1^{up} \mathbf{B}_{[1]}^\top \sin(\mathbf{B}_{[1]}\boldsymbol{\phi})$$
$$- \sigma R_1^{down} \mathbf{B}_{[2]} \sin(\mathbf{B}_{[2]}^\top \boldsymbol{\phi}). \quad (21)$$

The projected dynamics on nodes and triangles are now coupled by the modulation of the coupling constant σ with the order parameters R_1^{down} and R_1^{up}, i.e. the two projected phases follow the coupled dynamics

$$\dot{\boldsymbol{\phi}}^{[-]} = \mathbf{B}_{[1]}\tilde{\boldsymbol{\omega}} - \sigma R_1^{up} \mathbf{L}_{[0]} \sin \boldsymbol{\phi}^{[-]},$$
$$\dot{\boldsymbol{\phi}}^{[+]} = \mathbf{B}_{[2]}^\top \tilde{\boldsymbol{\omega}} - \sigma R_1^{down} \mathbf{L}_{[2]}^{down} \sin \boldsymbol{\phi}^{[+]}.$$
$$(22)$$

This explosive higher-order topological Kuramoto model has been shown in Ref. [16] to lead to discontinuous synchronization model on different models of simplicial complexes and on clique complexes or real connectomes as well.

B. Higher-order topological Kuramoto model of coupled topological signals of different dimension

In this work we want to discuss the case in which topological signals of different dimensions are coupled together leading to an explosive synchronization transition. Specifically we focus on the coupling of the traditional Kuramoto model (Eq.(13)) to higher-order topological Kuramoto model defined for phases associated to the links (Eq.(17)). The coupling between these two dynamics is here performed considering the modulation of the coupling constant σ with the global order parameters of the node dynamics (defined in Eq. (15)) and the link dynamics (defined in Eq. (20)). Specifically, we consider two models denoted as Model 1 and Model 2. Model 1 couples the dynamics of the phases of the nodes $\boldsymbol{\theta}$ and of the links $\boldsymbol{\phi}$ according to the following dynamical equations

$$\dot{\boldsymbol{\theta}} = \boldsymbol{\omega} - \sigma R_1^{down} \mathbf{B}_{[1]} \sin(\mathbf{B}_{[1]}^\top \boldsymbol{\theta}), \quad (23)$$
$$\dot{\boldsymbol{\phi}} = \tilde{\boldsymbol{\omega}} - \sigma R_0 \mathbf{B}_{[1]}^\top \sin(\mathbf{B}_{[1]}\boldsymbol{\phi}) - \sigma \mathbf{B}_{[2]} \sin(\mathbf{B}_{[2]}^\top \boldsymbol{\phi}). \quad (24)$$

The projected dynamics for $\boldsymbol{\phi}^{[-]}$ and $\boldsymbol{\phi}^{[+]}$ then obey

$$\dot{\boldsymbol{\phi}}^{[-]} = \mathbf{B}_{[1]}\tilde{\boldsymbol{\omega}} - \sigma R_0 \mathbf{L}_{[0]} \sin \boldsymbol{\phi}^{[-]}, \quad (25)$$
$$\dot{\boldsymbol{\phi}}^{[+]} = \mathbf{B}_{[2]}^\top \tilde{\boldsymbol{\omega}} - \sigma \mathbf{L}_{[2]}^{down} \sin \boldsymbol{\phi}^{[+]}. \quad (26)$$

Therefore the projection on the nodes $\boldsymbol{\phi}^{[-]}$ of the phases $\boldsymbol{\phi}$ associated to the links (Eq. (25)) is coupled to the dynamics of the phases $\boldsymbol{\theta}$ (Eq. (23)) associated directly to nodes. However the projection on the triangles $\boldsymbol{\phi}^{[+]}$ of the phases $\boldsymbol{\phi}$ associated to the links is independent of $\boldsymbol{\phi}^{[-]}$ and of $\boldsymbol{\theta}$ as well. Model 2 also describes the coupled dynamics of topological signals defined on nodes and links but the adaptive coupling captured by the model is different. In this case the dynamical equations are taken to be

$$\dot{\boldsymbol{\theta}} = \boldsymbol{\omega} - \sigma R_1^{down} \mathbf{B}_{[1]} \sin(\mathbf{B}_{[1]}^\top \boldsymbol{\theta}), \quad (27)$$
$$\dot{\boldsymbol{\phi}} = \tilde{\boldsymbol{\omega}} - \sigma R_0 R_1^{up} \mathbf{B}_{[1]}^\top \sin(\mathbf{B}_{[1]}\boldsymbol{\phi})$$
$$- \sigma R_1^{down} \mathbf{B}_{[2]} \sin(\mathbf{B}_{[2]}^\top \boldsymbol{\phi}). \quad (28)$$

For Model 2 the projected dynamics for $\boldsymbol{\phi}^{[-]}$ and for $\boldsymbol{\phi}^{[+]}$ obey

$$\dot{\boldsymbol{\phi}}^{[-]} = \mathbf{B}_{[1]}\tilde{\boldsymbol{\omega}} - \sigma R_0 R_1^{up} \mathbf{L}_{[0]} \sin \boldsymbol{\phi}^{[-]}, \quad (29)$$
$$\dot{\boldsymbol{\phi}}^{[+]} = \mathbf{B}_{[2]}^\top \tilde{\boldsymbol{\omega}} - \sigma R_1^{down} \mathbf{L}_{[2]}^{down} \sin \boldsymbol{\phi}^{[+]}. \quad (30)$$

Therefore, as in Model 1 the dynamics of the projection $\boldsymbol{\phi}^{[-]}$ of the phases $\boldsymbol{\phi}$ associated to the links (Eq. (29))

is coupled to the dynamics of the phases $\boldsymbol{\theta}$ associated directly to nodes (Eq. (27)) and vice versa. Moreover the dynamics of the projection of the phases $\boldsymbol{\phi}$ on the triangles $\boldsymbol{\phi}^{[+]}$ (Eq. (30)) is now also coupled with the dynamics of $\boldsymbol{\phi}^{[-]}$ (Eq. (29)) and vice versa. Here and in the following we will use the convenient notation (using the parameter m) to indicate both models 1 and 2 with the same set of dynamical equations given by

$$\dot{\boldsymbol{\theta}} = \boldsymbol{\omega} - \sigma R_1^{down}\mathbf{B}_{[1]}\sin(\mathbf{B}_{[1]}^{\top}\boldsymbol{\theta}), \qquad (31)$$

$$\dot{\boldsymbol{\phi}} = \tilde{\boldsymbol{\omega}} - \sigma R_0\left(R_1^{up}\right)^{m-1}\mathbf{B}_{[1]}^{\top}\sin(\mathbf{B}_{[1]}\boldsymbol{\phi})$$
$$- \sigma\left(R_1^{down}\right)^{m-1}\mathbf{B}_{[2]}\sin(\mathbf{B}_{[2]}^{\top}\boldsymbol{\phi}), \qquad (32)$$

which reduce to Eqs. (24) for $m = 1$ and to Eqs. (28) for $m = 2$.

We make two very relevant observations:

- First, the proposed coupling between topological signals of different dimension can be easily extended to signals defined on higher-order simplices providing a very general scenario for coupled dynamical processes on simplicial complexes.

- Secondly, the considered coupled dynamics of topological signals defined on nodes and links can be also studied on networks with exclusively pairwise interactions where we assume that the number of simplices of dimension $n > 1$ is zero. Therefore in this specific case this topological dynamics can have important effects also on simple networks.

We have simulated Model 1 and Model 2 on two main examples of simplicial complex models: the configuration model of simplicial complexes [49] and the Network Geometry with Flavor [12, 13] (see Figure 3). In both models we observe an explosive synchronization of the topological signals associated to the nodes and to the links. However the two models display a notable difference. In Model 1 we observe a discontinuity for R_0 and R_1^{down} at a non-zero coupling constant $\sigma = \sigma_c$, however R_1^{up} follows an independent transition at zero coupling (see Figure 3 panels (a) and (c)). In Model 2, on the contrary all order parameters R_0, R_1^{down} and R_1^{up} display a discontinuous transition occurring for the same non zero value of the coupling constant $\sigma = \sigma_c$ (see Figure 3 panels (b) and (d)). This is a direct consequence of the fact that in Model 1 the adaptive coupling leading to discontinuous phase transition only couples the phases $\boldsymbol{\phi}^{[-]}$ and $\boldsymbol{\theta}$, while for Model 2 the coupling involves also the phases $\boldsymbol{\phi}^{[+]}$.

Additionally we studied both Model 1 and Model 2 on two real connectomes: the human connectome of Ref. [52] and the c. elegans connectome from Ref. [53] (see Figure 4). Interestingly also for these real datasets we observe that in Model 1 the explosive synchronization involves only the phases $\boldsymbol{\theta}$ and $\boldsymbol{\phi}^{[-]}$ while in Model 2 we observe that also $\boldsymbol{\phi}^{[+]}$ undergoes an explosive synchronization transition at the same value of the coupling constant

$\sigma = \sigma_c$. Note that the connectome of homo sapiens displays a very non-trivial dynamics and for observing the phase transition it is necessary to let the system equilibrate by considering very long time series.

IV. ANALYTIC TREATMENT OF THE COUPLED DYNAMICS OF NODES AND LINKS

A. Theoretical solution of the model

As mentioned earlier the higher-order topological Kuramoto model coupling the topological signals defined on nodes and on links can be defined on simplicial complexes and on networks as well. In this section we exploit this property of the dynamics to provide an analytical understanding of the synchronization transition on uncorrelated random network within the annealed network approximation. Using the Ott-Antonsen method [43] combined with the annealed approximation [42] we characterize the steady state of the coupled higher-order Kuramoto dynamics and compare the analytical results to simulations of the original model and of the annealed equations.

B. Annealed dynamics

The first step for providing an analytical understanding of the proposed coupled dynamics of nodes and links is to determine the equations that capture the dynamics in the annealed approximation. For the dynamics of the phases $\boldsymbol{\theta}$ associated to the nodes - Eq. (31)- it is possible to proceed as in the traditional Kuramoto model [42]. However the annealed approximation for the dynamics of the phases $\boldsymbol{\phi}$ defined in Eq. (32) needs to be discussed in detail as it is not directly reducible to previous results. For addressing this problem our aim is to directly define the annealed approximation for the dynamics of the projected variables $\boldsymbol{\phi}^{[-]}$ which, here and in the following are indicated as

$$\boldsymbol{\psi} = \boldsymbol{\phi}^{[-]}, \qquad (33)$$

in order to simplify the notation. Moreover we will indicate with $N = N_{[0]}$ the number of nodes in the network or in the simplicial complex skeleton. Here we focus on the model defined on networks, i.e. we assume that there are no simplices of dimension two. Consequently R_1^{up} acquires the trivial value $R_1^{up} = 1$ and Model 2 reduces to Model 1 that we consider in detail here. We notice that Eq. (25), valid for Model 1 can be written as

$$\dot{\boldsymbol{\psi}} = \mathbf{B}_{[1]}\tilde{\boldsymbol{\omega}} - \sigma R_0\mathbf{L}_{[0]}\sin(\boldsymbol{\psi}). \qquad (34)$$

This equation can be also written elementwise as

$$\dot{\psi}_i = \hat{\omega}_i + \sigma R_0\sum_{j=1}^{N} a_{ij}\left[\sin(\psi_j) - \sin(\psi_i)\right], \qquad (35)$$
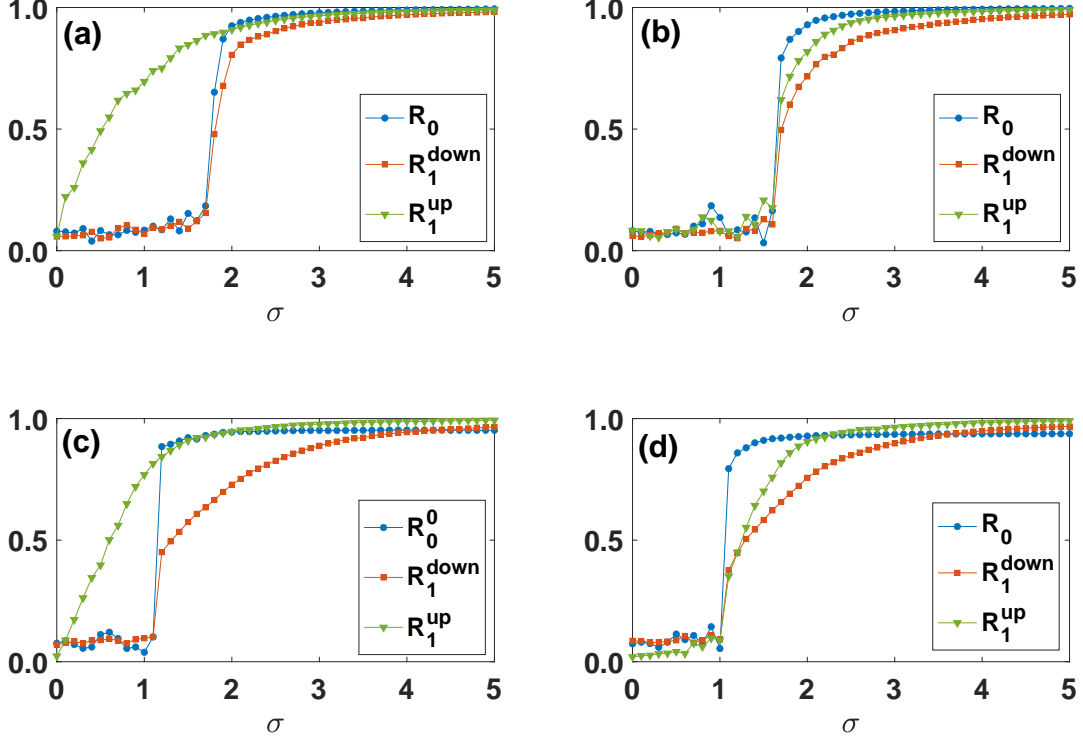
FIG. 3: **The Higher-order topological synchronization models (Models 1 and 2) coupling nodes and links on simplicial complexes.** The order parameters R_0, R_1^{down} and R_1^{up} are plotted versus σ for the higher-order topological synchronization Model 1 (panels (a) and (c)) and Model 2 (panels (b) and (d)) defined over the Network Geometry with Flavor [13] (panels (a) and (c)) and the configuration model of simplicial complexes [49] (panels (b) and (d)). The Network Geometry with Flavor on which we run the numerical results shown in (a) and (b) includes $N_{[0]} = 500$ nodes and has flavor $s = -1$ and $d = 3$. The configuration model of simplicial complexes on which we run the numerical results shown in (c) and (d) includes $N_{[0]} = 500$ nodes and has generalized degree distribution which is power-law with exponent $\gamma = 2.8$. In both Model 1 and in Model 2 we have set $\Omega_0 = \Omega_1 = 2$.

where the vector $\hat{\boldsymbol{\omega}}$ is given by

$$\hat{\omega} = \mathbf{B}_{[1]}\tilde{\boldsymbol{\omega}}. \tag{36}$$

Let us now consider in detail these frequencies in the case in which the generic internal frequency $\tilde{\omega}_\ell$ of a link follows a Gaussian distribution, specifically in the case in which $\tilde{\omega}_\ell \sim \mathcal{N}(\Omega_1, 1)$ for every link ℓ. Using the definition of the boundary operator on a link it is easy to show that the expectation of $\hat{\omega}_i$ is given by

$$\langle\hat{\omega}_i\rangle = \left[\sum_{j<i} a_{ij} - \sum_{j>i} a_{ij}\right]\Omega_1. \tag{37}$$

Given that each node has degree k_i, the covariance matrix $\mathbf{C}$ is given by the graph Laplacian $\mathbf{L}_{[0]}$ of the network, i.e.

$$\begin{aligned}C_{ij} &= \langle\hat{\omega}_i\hat{\omega}_j\rangle_c = \sum_{\ell,\ell'}\langle[\mathbf{B}_{[1]}\tilde{\boldsymbol{\omega}}]_i[\mathbf{B}_{[1]}\tilde{\boldsymbol{\omega}}]_j\rangle_c \\ &= [L_{[0]}]_{ij} = k_i\delta_{ij} - a_{ij}, \tag{38}\end{aligned}$$

where we have indicated with $\langle\ldots\rangle_c$ the connected correlation. Therefore the variance of $\hat{\omega}$ in the MF approximation is

$$\langle\hat{\omega}_i^2\rangle_c = \langle\hat{\omega}_i^2\rangle - \langle\hat{\omega}_i\rangle^2 = k_i. \tag{39}$$

Moreover, the projected frequencies are actually correlated and for $i \neq j$ we have

$$\langle\hat{\omega}_i\hat{\omega}_j\rangle_c = \langle\hat{\omega}_i\hat{\omega}_j\rangle - \langle\hat{\omega}_i\rangle\langle\hat{\omega}_j\rangle = -a_{ij}. \tag{40}$$

It follows that the frequencies $\hat{\boldsymbol{\omega}}$ are correlated Gaussian variables with average given by Eq. (37) and correlation matrix given by the graph Laplacian. Here and in the following we will denote by $G(\hat{\boldsymbol{\omega}})$ the distribution of these frequencies. The fact that the frequencies $\hat{\omega}_i$ are correlated is an important feature of the dynamics of $\boldsymbol{\psi}$ and, with few exceptions (e.g., [54]), this feature has remained relatively unexplored in the case of the standard Kuramoto model. Additionally let us note that the average of $\hat{\omega}$ over all the nodes of the network is zero. In
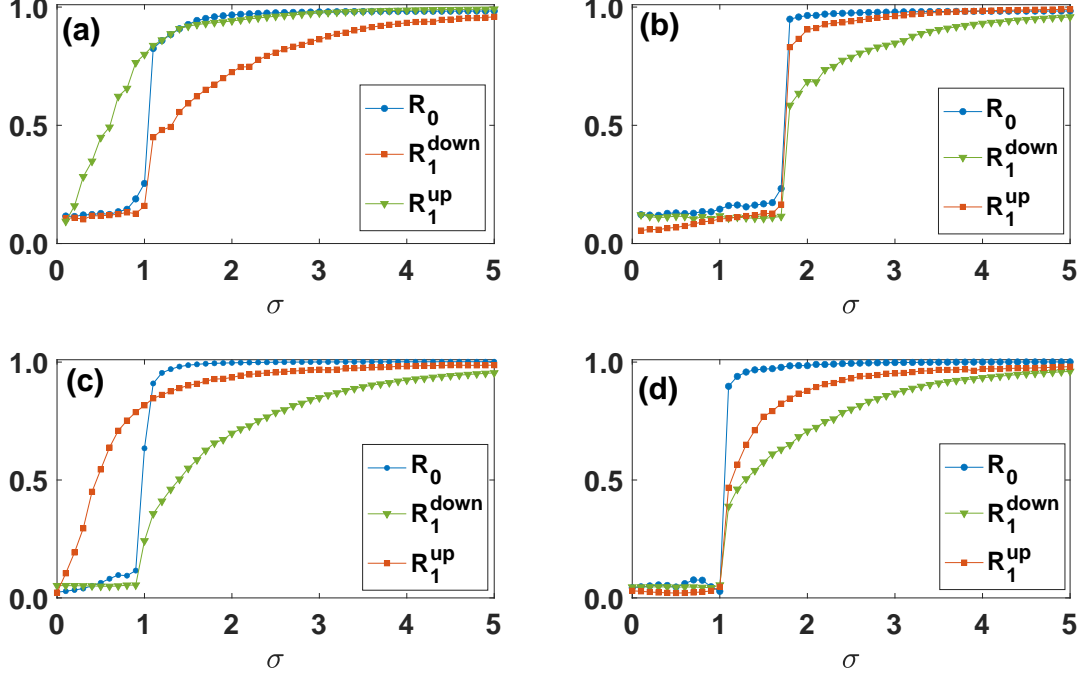
FIG. 4: **The Higher-order topological synchronization models (Models 1 and 2) coupling nodes and links on real connectomes.** The order parameters R_0, R_1^{down} and R_1^{up} are plotted versus σ on real connectomes. Panel (a) and (b) show the numerical results on the human connectome [52] for Model 1 and Model 2 respectively. Panel (c) and (d) show the numerical results on the c. elegans connectome [53] for Model 1 and Model 2 respectively. In both Model 1 and in Model 2 we have set $\Omega_0 = \Omega_1 = 2$.

fact

$$\sum_{i=1}^{N} \hat{\omega}_i = \mathbf{1}^T \hat{\boldsymbol{\omega}} = \mathbf{1}^T \mathbf{B}_{[1]} \boldsymbol{\omega} = 0, \tag{41}$$

where with $\mathbf{1}$ we indicate the N-dimensional column vector of elements $1_i = 1$. By using the symmetry of the adjacency matrix, i.e. the fact that $a_{ij} = a_{ji}$, Eq. (41) implies that the sum of $\dot{\psi}_i$ over all the nodes of the network is zero, i.e.

$$\sum_{i=1}^{N} \dot{\psi}_i = \sum_{i=1}^{N} \hat{\omega}_i + \sigma R_0 \sum_{i,j} a_{ij} [\sin(\psi_j) - \sin(\psi_i)] = 0.$$

We now consider the annealed approximation consisting in substituting the adjacency matrix element a_{ij} with its expectation in an uncorrelated network ensemble

$$a_{ij} \to \frac{k_i k_j}{\langle k \rangle N}, \tag{42}$$

where k_i indicates the degree of node i and $\langle k \rangle$ is the average degree of the network. In the annealed approximation we can put

$$\langle \hat{\omega}_i \rangle \simeq k_i \Omega_1 \left[1 - 2 \sum_{j>i} \frac{k_j}{\langle k \rangle N} \right]. \tag{43}$$

Also, in the annealed approximation the dynamical Eq. (31) and Eq. (34) reduce to

$$\dot{\boldsymbol{\theta}} = \boldsymbol{\omega} - \sigma R_1^{down} \hat{R}_0 \mathbf{k} \cdot \sin(\boldsymbol{\theta} - \Theta), \tag{44}$$

$$\dot{\boldsymbol{\psi}} = \hat{\boldsymbol{\omega}} + \sigma R_0 \hat{R}_1^{down} \mathbf{k} \sin \Psi - \sigma R_0 \mathbf{k} \odot \sin \boldsymbol{\psi}, \tag{45}$$

where $\odot$ indicates the Hadamard product (element by element multiplication) and where two additional complex order parameters are defined as

$$\hat{R}_0 e^{\mathrm{i}\Theta} = \sum_{i=1}^{N} \frac{k_i}{\langle k \rangle N} e^{\mathrm{i}\theta_i},$$

$$\hat{R}_1^{down} e^{\mathrm{i}\Psi} = \sum_{i=1}^{N} \frac{k_i}{\langle k \rangle N} e^{\mathrm{i}\psi_i}. \tag{46}$$

C. Solution of the dynamical equations in the annealed approximation

1. General framework for obtaining the solution of the annealed dynamical equations

In this section we will provide the analytic solutions for the order parameter of the higher-order topological

synchronization studied within the annealed approximation, i.e., captured by Eqs. (44) and (45). In particular first we will find an expression of the order parameters R_0 of the dynamics associated to the nodes (Eq. (44)) and subsequently in the next paragraph we will derive the expression for the order parameter R_1^{down} associated to the projection on the nodes of the topological signal defined on the links (Eq. 45)). By combining the two results it is finally possible to uncover the discontinuous nature of the transition.

2. Dynamics of the phases of the nodes

When we investigate Eq. (44) we notice that this equation can be easily reduced to the equation for the standard Kuramoto model treated within the annealed approximation [42] if one performs a rescaling of the coupling constant $\sigma R_0 \to \sigma$. Therefore we can treat this model similarly to the known treatment of the standard Kuramoto model [40–42]. Specifically, starting from Eq. (44) and using a rescaling of the phases $\boldsymbol{\theta}$ according to

$$\theta_i \to \theta_i - \Omega_0 t, \tag{47}$$

it is possible to show that we can set $\Theta = 0$ and therefore Eq. (44) reduces to the well-known annealed expression for the standard order Kuramoto model given by

$$\dot{\boldsymbol{\theta}} = \boldsymbol{\omega} - \Omega_0 \mathbf{1} - \sigma R_1^{down} \hat{R}_0 \mathbf{k} \cdot \sin(\boldsymbol{\theta}). \tag{48}$$

Assuming that the system of equations reaches a steady state in which both R_1^{down} and $\hat{R}_0$ become time independent, the order parameters of this system of equations can be found to obey [40, 42, 48, 55]

$$\hat{R}_0 = \sum_{i=1}^N \frac{k_i}{\langle k \rangle N} \int_{|\hat{c}_i|<1} d\omega g(\omega) \sqrt{1 - \left(\frac{\omega - \Omega_0}{\sigma k_i \hat{R}_0 R_1^{down}}\right)^2},$$

$$R_0 = \frac{1}{N} \sum_{i=1}^N \int_{|\hat{c}_i|<1} d\omega g(\omega) \sqrt{1 - \left(\frac{\omega - \Omega_0}{\sigma k_i \hat{R}_0 R_1^{down}}\right)^2} \tag{49}$$

where c_i indicates

$$c_i = \frac{\omega - \Omega_0}{\sigma k_j \hat{R}_0 R_1^{down}}. \tag{50}$$

and $g(\omega)$ is the Gaussian distribution with expectation Ω_0 and standard deviation 1.

3. Dynamics of the phases of the links projected on the nodes

In this paragraph we will derive the expression of the order parameters R_1^{down} and $\hat{R}_1^{down}$ which, together with Eqs. (49), will provide the annealed solution of our model.

To start with we assume that the frequencies $\hat{\boldsymbol{\omega}}$ are known. In this case we can express the order parameters R_1^{down} and $\hat{R}_1^{down}$ as a function of the probability density function $\rho^{(i)}(\psi, t|\hat{\boldsymbol{\omega}})$ that node i is associated to a projected phase of the link equal to ψ. Since in the annealed approximation ψ_i has a dynamical evolution dictated by Eq. (45) the probability density function obeys the continuity equation

$$\partial_t \rho^{(i)}(\psi, t|\hat{\boldsymbol{\omega}}) + \partial_\psi \left[\rho^{(i)}(\psi, t|\hat{\boldsymbol{\omega}})) v_i\right] = 0 \tag{51}$$

with associated velocity v_i given by

$$v_i = \kappa_i - \sigma R_0 k_i \sin \psi \tag{52}$$

where we have defined κ_i as

$$\kappa_i = \hat{\omega}_i + \sigma k_i R_0 \hat{R}_1^{down} \sin \Psi. \tag{53}$$

In this case the complex order parameters are given by

$$\hat{R}_1^{down} e^{\mathring{\imath}\Psi} = \sum_{i=1}^N \frac{k_i}{\langle k \rangle N} \int d\psi \rho^{(i)}(\psi, t|\hat{\boldsymbol{\omega}}) e^{\mathring{\imath}\psi}$$

$$R_1^{down} e^{\mathring{\imath}\tilde{\Psi}} = \sum_{i=1}^N \frac{1}{N} \int d\psi \rho^{(i)}(\psi, t|\hat{\boldsymbol{\omega}}) e^{\mathring{\imath}\psi} \tag{54}$$

In order to solve the continuity equation we follow Ott-Antonsen [43] and we express $\rho^{(i)}(\psi, t|\hat{\boldsymbol{\omega}})$ in the Fourier basis as

$$\rho^{(i)}(\psi, t|\hat{\boldsymbol{\omega}}) = \frac{1}{2\pi} \left\{1 + \sum_{m=1}^\infty \hat{f}_m^{(i)}(\hat{\omega}_i, t) e^{\mathring{\imath}m\psi} + c.c.\right\}. \tag{55}$$

Making the ansatz

$$\hat{f}_m^{(i)}(\hat{\omega}_i, t) = [b_i(\hat{\omega}_i, t)]^m \tag{56}$$

we can derive the equation for the evolution of $b_i = b_i(\hat{\omega}_i, t)$ given by

$$\partial_t b_i + \mathring{\imath} b_i \kappa_i + \sigma k_i R_0 \frac{1}{2}(b_i^2 - 1) = 0. \tag{57}$$

Since we showed before that the average value of $\dot{\psi}_i$ over nodes is zero, we look for non-rotating stationary solutions of Eq. (57), $\partial_t b_i = 0$, given by

$$b_i = -\mathring{\imath} d_i \pm \sqrt{1 - d_i^2}, \tag{58}$$

where d_i is given by

$$d_i = \frac{\hat{\omega}_i}{\sigma k_i R_0} + \hat{R}_1^{down} \sin \Psi. \tag{59}$$

By plugging this expression into Eq. (54) we get the expression of the order parameters given the projected frequencies $\hat{\boldsymbol{\omega}}$,

$$\hat{R}_1^{down}\cos\Psi \;=\; \sum_{i=1}^{N}\frac{k_i}{\langle k\rangle N}\sqrt{1-d_i^2}\,\theta(1-d_i^2)$$

$$\hat{R}_1^{down}\sin\Psi \;=\; \sum_{i=1}^{N}\frac{k_i}{\langle k\rangle N}\left\{\sqrt{d_i^2-1}\,\chi(d_i)+d_i\right\}$$

$$R_1^{down} \;=\; \frac{1}{N}\left|\sum_{i=1}^{N}d_i-\mathrm{sign}(d_i+1)\sqrt{d_i^2-1}\right| \quad (60)$$

where, indicating by $\theta(x)$ the Heaviside function, we have defined

$$\chi(d_i)=[-\theta(d_i-1)+\theta(-1-d_i)]. \qquad (61)$$

Finally, if the projected frequencies $\hat{\boldsymbol{\omega}}$ are not known we can average the result over the frequency distribution $G(\hat{\boldsymbol{\omega}})$ getting

$$\hat{R}_1^{down}\cos\Psi \;=\; \sum_{i=1}^{N}\frac{k_i}{\langle k\rangle N}\int_{|d_i|\le 1}d\hat{\boldsymbol{\omega}}\,G(\hat{\boldsymbol{\omega}})\sqrt{1-\left(\frac{\hat{\omega}_i}{\sigma R_0 k_i}+\hat{R}_1^{down}\sin\Psi\right)^2},$$

$$\hat{R}_1^{down}\sin\Psi \;=\; -\sum_{j=0}^{N}\frac{k_i}{\langle k\rangle N}\int_{d_i>1}d\hat{\boldsymbol{\omega}}\,G(\hat{\boldsymbol{\omega}})\sqrt{\left(\frac{\hat{\omega}_i}{\sigma R_0 k_i}+\hat{R}_1^{down}\sin\Psi\right)^2-1}$$

$$+\sum_{i=1}^{N}\frac{k_i}{\langle k\rangle N}\int_{d_i<-1}d\hat{\boldsymbol{\omega}}\,G(\hat{\boldsymbol{\omega}})\sqrt{\left(\frac{\hat{\omega}_i}{\sigma R_0 k_i}+\hat{R}_1^{down}\sin\Psi\right)^2-1}$$

$$+\sum_{i=1}^{N}\frac{k_i}{\langle k\rangle N}\int_{-\infty}^{\infty}d\hat{\boldsymbol{\omega}}\,G(\hat{\boldsymbol{\omega}})\left(\frac{\hat{\omega}_i}{\sigma R_0 k_i}+\hat{R}_1^{down}\sin\Psi\right), \qquad (62)$$

and

$$R_1^{down}=\frac{1}{N}\left|\sum_{i=1}^{N}\int_{-\infty}^{\infty}d\hat{\boldsymbol{\omega}}\,G(\hat{\boldsymbol{\omega}})\left(\frac{\hat{\omega}_i}{\sigma R_0 k_i}+\hat{R}_1^{down}\sin\Psi-\mathrm{sign}(d_i+1)\sqrt{\left(\frac{\hat{\omega}_i}{\sigma R_0 k_i}+\hat{R}_1^{down}\sin\Psi\right)^2-1}\right)\right|. \qquad (63)$$

By solving these equations together with Eqs. (49) we can capture the critical behavior of the higher-order Kuramoto model coupling topological signals defined on nodes and links within the annealed approximation.

In Figure 5 we compared the direct numerical integration of the annealed Eqs. (44) and (45) with the obtained theoretical predictions finding very good agreement. This derivation therefore shows evidence of the discontinuous nature of the observed dynamics. However we have found that the annealed approximation of the considered model captures the critical point σ_c of the transition but is otherwise not a very controllable approximation of the original higher-order topological dynamics at least for the moderately small network sizes that can be considered numerically.

V. CONCLUSIONS

Until recently the synchronization phenomenon has been explored only in the context of topological signals associated to the nodes of a network. However the growing interest in simplicial complexes opens the perspective of investigating synchronization of higher order topological signals, for instance associated to the links of the discrete networked structure. Here we uncover how topological signals associated to nodes and links can be coupled to one another giving rise to an explosive synchronization phenomenon involving both signals at the same time. The model has been tested on real connectomes and on major examples of simplicial complexes (the configuration model [49] of simplicial complex and the Network Geometry with Flavor[13]). Moreover we
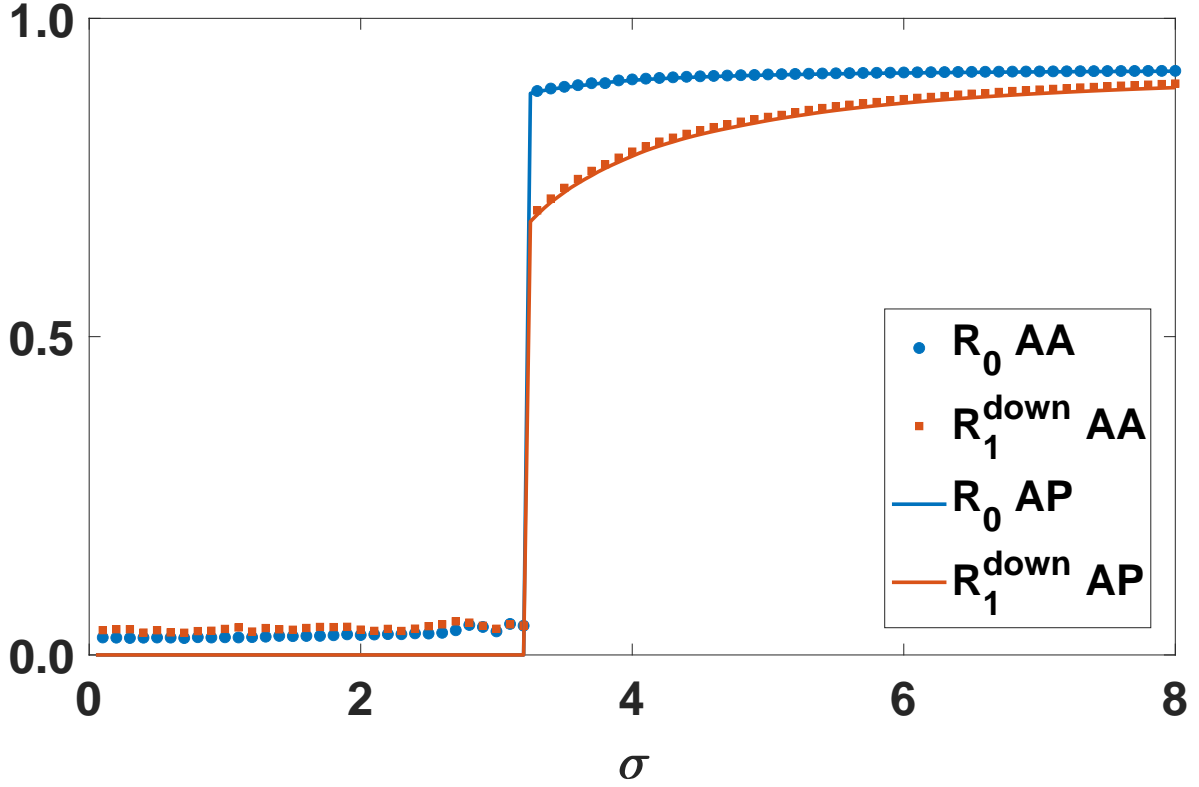
FIG. 5: **The discontinuous phase transition obtained in the annealed approximation** The order parameters R_0 (circles) and R_1^{down} (squares) are plotted as a function of the coupling constant σ for the annealed approximation (AA) dynamics. The solid lines indicate the analytical predictions (AP) obtained in this approximation. Simulations (AA) are here obtained by integrating numerically Eqs. (44) and (45) for a Poisson network of $N = 1000$ nodes and average degree $c = 2.5$.

provide an analytical solution of this model within the annealed approximation that provides a theoretical understanding of the mechanism driving the emergence of this discontinuous phase transition. This work can be extended in different directions including the study of the de-synchronization dynamics of this coupled higher-order synchronization and the duality of this model with the same model defined on the line graph of the same network.

Acknowledgements

[1] C. Giusti, R. Ghrist, and D. S. Bassett, Journal of computational neuroscience **41**, 1 (2016).

[2] F. Battiston, G. Cencetti, I. Iacopini, V. Latora, M. Lucas, A. Patania, J.-G. Young, and G. Petri, Physics Reports (2020).

[3] L. Torres, A. S. Blevins, D. S. Bassett, and T. Eliassi-Rad, arXiv preprint arXiv:2006.02870 (2020).

[4] V. Salnikov, D. Cassese, and R. Lambiotte, European Journal of Physics **40**, 014001 (2018).

[5] N. Otter, M. A. Porter, U. Tillmann, P. Grindrod, and

H. A. Harrington, EPJ Data Science **6**, 17 (2017).

[6] G. Petri, M. Scolamiero, I. Donato, and F. Vaccarino, PloS one **8**, e66506 (2013).

[7] G. P. Massara, T. Di Matteo, and T. Aste, Journal of complex Networks **5**, 161 (2016).

[8] R. Sreejith, K. Mohanraj, J. Jost, E. Saucan, and A. Samal, Journal of Statistical Mechanics: Theory and Experiment **2016**, 063206 (2016).

[9] A. P. Kartun-Giles and G. Bianconi, Chaos, Solitons & Fractals: X **1**, 100004 (2019).

[10] J. W. Rocks, A. J. Liu, and E. Katifori, Physical Review Research **2**, 033234 (2020).

[11] Z. Wu, G. Menichetti, C. Rahmede, and G. Bianconi, Scientific reports **5**, 1 (2015).

[12] G. Bianconi and C. Rahmede, Scientific reports **7**, 41974 (2017).

[13] G. Bianconi and C. Rahmede, Physical Review E **93**, 032315 (2016).

[14] M. M. Dankulov, B. Tadić, and R. Melnik, Physical Review E **100**, 012309 (2019).

[15] B. Tadić, M. Andjelković, and R. Melnik, Scientific reports **9**, 1 (2019).

[16] A. P. Millán, J. J. Torres, and G. Bianconi, Physical Review Letters **124**, 218301 (2020).

[17] J. J. Torres and G. Bianconi, Journal of Physics: Complexity **1**, 015002 (2020).

[18] M. Reitz and G. Bianconi, Journal of Physics A: Mathematical and Theoretical (2020).

[19] S. Barbarossa and S. Sardellitti, IEEE Transactions on Signal Processing (2020).

[20] N. Landry and J. G. Restrepo, arXiv preprint arXiv:2006.15453 (2020).

[21] P. S. Skardal and A. Arenas, Physical review letters **122**, 248301 (2019).

[22] P. S. Skardal and A. Arenas, arXiv preprint arXiv:1909.08057 (2019).

[23] I. Iacopini, G. Petri, A. Barrat, and V. Latora, Nature communications **10**, 1 (2019).

[24] D. Taylor, F. Klimm, H. A. Harrington, M. Kramár, K. Mischaikow, M. A. Porter, and P. J. Mucha, Nature communications **6**, 1 (2015).

[25] M. Lucas, G. Cencetti, and F. Battiston, Physical Review Research **2**, 033410 (2020).

[26] Y. Zhang, V. Latora, and A. E. Motter, arXiv preprint arXiv:2010.00613 (2020).

[27] P. S. Skardal and A. Arenas, Journal of Physics: Complexity (2020).

[28] L. DeVille, arXiv preprint arXiv:2010.07421 (2020).

[29] T. Carletti, D. Fanelli, and S. Nicoletti, arXiv preprint arXiv:2006.01243 (2020).

[30] A. P. Millán, J. J. Torres, and G. Bianconi, Scientific Reports **8**, 1 (2018).

[31] R. Mulas, C. Kuehn, and J. Jost, arXiv preprint arXiv:2003.13775 (2020).

[32] L. Gambuzza, F. Di Patti, L. Gallo, S. Lepri, M. Romance, R. Criado, M. Frasca, V. Latora, and S. Boccaletti, arXiv preprint arXiv:2004.03913 (2020).

[33] A. P. Millán, J. J. Torres, and G. Bianconi, Phys. Rev. E **99**, 022307 (2019).

[34] F. P. U. Severino, J. Ban, Q. Song, M. Tang, G. Bianconi, G. Cheng, and V. Torre, Scientific reports **6**, 29640 (2016).

[35] M. Saggar, O. Sporns, J. Gonzalez-Castillo, P. A. Bandettini, G. Carlsson, G. Glover, and A. L. Reiss, Nature communications **9**, 1 (2018).

[36] C. Giusti, E. Pastalkova, C. Curto, and V. Itskov, Proceedings of the National Academy of Sciences **112**, 13455 (2015).

[37] M. W. Reimann, M. Nolte, M. Scolamiero, K. Turner, R. Perin, G. Chindemi, P. Dłotko, R. Levi, K. Hess, and H. Markram, Frontiers in computational neuroscience **11**, 48 (2017).

[38] M. Ruiz-Garcia and E. Katifori, arXiv preprint arXiv:2001.01811 (2020).

[39] S. H. Strogatz, Physica D: Nonlinear Phenomena **143**, 1 (2000).

[40] S. Boccaletti, A. N. Pisarchik, C. I. Del Genio, and A. Amann, *Synchronization: from coupled systems to complex networks* (Cambridge University Press, 2018).

[41] F. A. Rodrigues, T. K. D. Peron, P. Ji, and J. Kurths, Physics Reports **610**, 1 (2016).

[42] J. G. Restrepo, E. Ott, and B. R. Hunt, Physical Review E **71**, 036151 (2005).

[43] E. Ott and T. M. Antonsen, Chaos: An Interdisciplinary Journal of Nonlinear Science **18**, 037113 (2008).

[44] W. Huang, T. A. Bolton, J. D. Medaglia, D. S. Bassett, A. Ribeiro, and D. Van De Ville, Proceedings of the IEEE **106**, 868 (2018).

[45] T. S. Evans and R. Lambiotte, The European Physical Journal B **77**, 265 (2010).

[46] R. M. D'Souza, J. Gómez-Gardeñes, J. Nagler, and A. Arenas, Advances in Physics **68**, 123 (2019).

[47] X. Zhang, S. Boccaletti, S. Guan, and Z. Liu, Physical review letters **114**, 038701 (2015).

[48] S. Boccaletti, J. Almendral, S. Guan, I. Leyva, Z. Liu, I. Sendiña-Nadal, Z. Wang, and Y. Zou, Physics Reports **660**, 1 (2016).

[49] O. T. Courtney and G. Bianconi, Physical Review E **93**, 062311 (2016).

[50] R. W. Ghrist, *Elementary applied topology*, Vol. 1 (Createspace Seattle, 2014).

[51] D. Horak and J. Jost, Advances in Mathematics **244**, 303 (2013).

[52] P. Hagmann, L. Cammoun, X. Gigandet, R. Meuli, C. J. Honey, V. J. Wedeen, and O. Sporns, PLoS Biol **6**, e159 (2008).

[53] L. R. Varshney, B. L. Chen, E. Paniagua, D. H. Hall, and D. B. Chklovskii, PLoS Comput Biol **7**, e1001066 (2011).

[54] P. S. Skardal, J. G. Restrepo, and E. Ott, Physical Review E **91**, 060902 (2015).

[55] T. Ichinomiya, Physical Review E **70**, 026116 (2004).